

Electrochemical Fabrication of Pseudo Platinum Foam and its Application in Methanol Electrooxidation

Hongdan Wang^{1,2}, Liqiu Zhang², Hongxia Shen², Lichun Liu^{1,2*}, and Lihua Li^{1*}

¹ College of Petroleum Engineering, Liaoning Shihua University, Fu Shun, Liaoning Province, 113000, People's Republic of China

² College of Biological, Chemical Sciences and Engineering, Jiaying University, Jiaying, Zhejiang Province, 314001, People's Republic of China

*E-mail: lichun.liu@mail.zjxu.edu.cn, llh72@163.com

Received: 13 September 2017 / Accepted: 18 October 2017 / Published: 12 November 2017

Porous non-noble metal foams find many industrial applications, however applications of noble metal platinum (Pt) foams were scarce. In this work, we demonstrate a successful fabrication of a pseudo Pt foam by electrochemically coating Pt onto a Ni foam template. A thin ~55 nm Pt layer was electrochemically deposited on a Ni foam with a solution consisting of a low concentration of chloroplatinic acid (H₂PtCl₆) and polyvinyl pyrrolidone (PVP) additive, using cyclic voltametric deposition technique (-0.3 ~ 0 V vs Ag/AgCl). PVP played a critical role in forming a thin and compact Pt layer. The fabricated pseudo Pt foams were free from cracks and presented good stability in acidic solution. The pseudo Pt foams contained trace amount of Pt, and exhibited typical chemical properties of metallic Pt and high surface area same as Ni foam base. With the application of as obtained Pt foam as a catalyst for methanol electrooxidation, the mass-specific current obtained is comparable to the commercial Pt/C electrocatalyst. The as-fabricated three-dimensional interconnected porous Pt foams may find versatile electrochemical applications as cost-effective working electrodes or auxiliary electrodes, in fuel cells, (dye sensitized solar cells) DSSCs, sensors, supercapacitors, and so on.

Keywords: Pt foam; Ni foam; fuel cell; methanol; electrodeposition; PVP

1. INTRODUCTION

Metal foams are porous metallic materials with open cells and interconnected network with high porosity, i.e. typically 75-95% of the volume consists of void spaces. Besides retaining the same chemical properties as their base metals, metallic foams bear extraordinary physical features including lightweight, high surface area, and excellent mechanical and energy absorptive properties [1]. These

make them suitable for numerous industrial applications, such as filtration, sound absorption, magnetic shielding, vibration damping, thermal insulation barriers, medical implants, storage media, electrodes, catalysts, and heat exchangers [2, 3]. Until now, non-noble metal foams (Ni, Cu, Al, etc.) are popular in most of these applications owing to the low cost and mature production technologies [4]. In contrast, noble metal foams are less used in practical scenarios, primarily due to the high production costs in conventional methods, such as gas bubbling and polymeric template assisted electrodeposition [5]. Thus, developing affordable, low cost noble metal foams is extremely significant owing to its use in many applications, especially those used in harsh corrosive environments.

Pt as one of the most popular noble metals is extensively used in chemical catalysis, corrosion protection, electrochemical energy conversion and as an auxiliary electrode [6]. Theoretically, Pt foam can be fabricated in the same manner as other non-noble metal foams. However, since the conventional production methods of non-noble metal foams are usable for fabricating large-ligament ($>1 \mu\text{m}$) foams, their application in fabricating Pt foams will consume large quantity of Pt metal, resulting in high material cost and impracticality. However, one key point which should be noted is that in many chemical applications only surface Pt atoms can take effect. Thus, to prepare a thin Pt layer on an inexpensive non-noble metal foam is reasonable for functioning as a Pt foam. Such pseudo Pt foam can reduce the usage of expensive Pt metal as compared to pure Pt foam. A similar concept has been practiced by Li et al. who fabricated Pt monolayer coating on Au coated Ni foam [7]. This report aimed to minimize the Pt usage for practical applications, but the high cost of Au buffer layer was not considered. Therefore, in real terms, the total cost was not only due to Pt but Au. Additionally, the fabrication process was complex and time consuming. In another work, Yamauchi et al. have fabricated Pt nanoparticles on Ni foam using lyotropic liquid crystalline template [8]. Porous Pt nanoparticles film was deposited on Ni foam through a replacement reaction. However, the stability of such composite was not investigated. In certain applications, the corrosive solution may penetrate into Ni foam through the internal pores of Pt nanoparticles film and destroy the whole structure.

To address the above-mentioned issues, in this work, we aimed to use a wet-chemical processing technique to electrochemically deposit a thin layer of Pt on an ordinary Ni foam to fabricate pseudo Pt foams. Through experimental trials, crack-free Pt coating as thin as $\sim 55 \text{ nm}$ was successfully deposited on Ni foam by cyclic voltametric electrodeposition process. Pseudo Pt foam exhibited all the electrochemical features of an ordinary Pt electrode. The long-term stability of as-fabricated Pt foam in acidic solution showed excellent results over a period of 10 days. Notably, its application as direct methanol fuel cell electrode exhibits similar mass specific catalytic current as a commercial Pt/C nanocomposite electrocatalyst. The as-fabricated cost-effective Pt foam holds great potential in practical electrochemical applications.

2 EXPERIMENTAL

2.1 Chemicals

Chloroplatinic acid (H_2PtCl_6), polyvinyl pyrrolidone (PVP, K-30, MW40000), methanol, sulfuric acid (H_2SO_4), sodium hydroxide (NaOH), sodium sulfate (Na_2SO_4) were purchased from

Tansoole Technology, China. Pt/C (5% mass ratio) was purchased from Adamas-beta, China. All chemicals were of analytical reagent grade. The aqueous solutions were prepared with deionized (DI) water.

2.2 Instruments

All electrochemical experiments were conducted on an electrochemical workstation P4000 (Princeton Applied Research, USA) equipped with Pt mesh counter electrode and Ag/AgCl (3 M KCl) reference electrode. The morphologies of the foams were observed using Field Emission Scanning Electron Microscopy (FESEM, Hitachi S-4800, Japan) operated at proper accelerating voltages. The mass of Pt loaded on Ni foam was evaluated by using Inductively Coupled Plasma Atomic Emission Spectroscopy (ICP-AES, IRIS Intrepid, Thermo Fisher, America).

2.3 Methods

Ni foam was cut into the size of 30*5*2 mm. To remove the surface impurities and oxide layers on a piece of Ni foam, pretreatment was performed by immersing in acetone, 0.5 M HCl, and ethanol under sonication for 30 minutes, respectively. Finally, Ni foams were rinsed with ethanol for three times, dried in vacuum at 60 °C for 1 hour and then stored in vacuum for further use.

Prior to use of pretreated Ni foam, insulating ceresin was melted and cast into Ni foam to avoid syphonage of the solution which influences electrodeposition and electrochemical characterization. After solidification of ceresin by cooling down to room temperature, a strip of Ni foam was carefully cut keeping 2 mm length from the one end to the ceresin block as working part.

Commercial Pt/C modified electrode was prepared by dispersing 10 mg Pt/C in 1 mL ethanol by ultrasonication and then dropped 5 μ L solution on a glassy carbon electrode (ϕ , 2 mm). After drying the electrode in room temperature for 20 minutes, 10 μ L Nafion (0.5% ethanol solution) was further dropped on the glassy carbon electrode to immobilize Pt/C to the electrode surface. After complete ethanol evaporation at room temperature, the Pt/C modified glassy carbon electrode was used to collect electrochemical data, on which Pt mass was about 2.5 μ g.

Pt mass in a Pt foam was obtained by monitoring the concentration of H_2PtCl_6 in the solution by ICP technique before and after electrodeposition. For 50 cycle electrodeposition, Pt mass in Pt foam was about 52 μ g.

3. RESULTS AND DISCUSSION

3.1 Direct Pt Electrodeposition

Hexachloroplatinic acid (H_2PtCl_6), being one of the most commonly used Pt precursor compounds, was used to produce metallic Pt in this work. H_2PtCl_6 releases PtCl_6^{2-} complex ions in an aqueous solution at room temperature [9, 10]. In a typical deposition procedure, thin Pt coating was

formed on Ni foam by applying cyclic voltammetric scan (-0.3 ~ 0 V vs Ag/AgCl) using an electrolyte containing 3 mM H_2PtCl_6 at room temperature. This concentration was optimized by considering the deposition rate, cost, and the feasibility of the spontaneous replacement reaction. Higher concentration can accelerate the rate of deposition but consume larger amounts of the expensive Pt compound. On the other hand, lower concentration of H_2PtCl_6 results in longer deposition time. The concentration of H_2PtCl_6 was determined at a moderate low concentration, i.e. 3mM. This concentration of H_2PtCl_6 was also sufficient to significantly decelerate the rate of reaction associated with the spontaneous replacement reaction that occurs vigorously when Ni foam is brought into contact with a high-concentration H_2PtCl_6 solution due to the large difference in their reduction potentials (0.74 V for $\text{PtCl}_6^{2+}/\text{Pt}$ [11] and -0.26 V for Ni/Ni^{2+} [12]). In addition, diffusion of ions in the solution is normally accompanied with electrochemical reactions. When the electrodeposition of Pt starts on Ni foam, PtCl_6^{2-} ions diffuse towards the surface of Ni foam. Due to three-dimensional porous structure of Ni foam, initially, ions in the bulk solution reach the outer surface and subsequently migrate towards its inner surface, forming an ionic gradient. This will cause a larger amount of Pt to deposit on the outer surface leading to an inhomogeneous coating. To overcome this problem, cyclic voltammetric deposition was adopted, which was helpful for maintaining a homogeneous concentration of PtCl_6^{2-} ions, both inside and outside the Ni foam. Since electrodeposition did not occur at the more positive potential range cyclic voltammetry allowed longer time for diffusion of ample quantities of ions.

3.2 Electrochemical characterization of cracks in the Pt coating

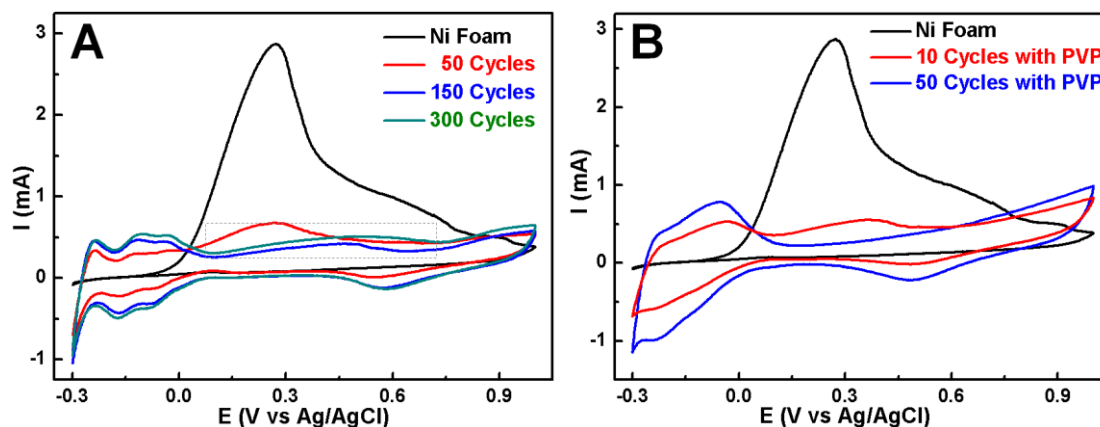


Figure 1. (A) Cyclic voltammograms for Ni foam (black), Pt deposited 50 (red), 150 (blue), and 300 (green) cycles on Ni foam. (B) Cyclic voltammograms for Ni foam (black), Pt deposited 50 cycles (red) from solution containing 0.15 mM PVP and 3 mM H_2PtCl_6 . CV curves were obtained using in 0.1 M H_2SO_4 electrolyte at 100 mV/s scan rate. (For clarity, not all CV curves collected in the experiment are included in the Figures)

Since electrochemical reactions usually take place on the surface of an electrode, electrochemical characterization is applicable to investigate about the coverage of the surface of Ni foam by Pt layer. Cyclic voltammetry was conducted to investigate the changes on the surface during the process of electrodeposition. Figure 1A shows cyclic voltammograms conducted in 0.1 M H_2SO_4 for

Ni foam (black trace), and Pt coated Ni foam deposited for 50 (red curve), 150 (blue curve), and 300 (green curve) cycles. It is obvious that the peak at 0.27 V (black curve) corresponds to the electrochemical oxidation of exposed Ni foam. When Pt was electrodeposited on Ni foam, the oxidation peak of Ni was suppressed as a function of amount of deposited Pt (red, blue, green curves). Although Ni oxidation peak was significantly suppressed with an increase in the number of coating cycles for Pt coating, a weak broad peak still appeared between 0 – 0.7 V in the CV curves as indicated by dashed rectangle in Figure 1A. This type of peak existed even Pt was deposited for up to 300 cycles using 3 mM H_2PtCl_6 solution (green curve) and could be attributed to the cracks that existed in Pt coating as evidenced in Figure 2A.

3.3 PVP assisted electrodeposition for obtaining crack-free Pt foam

Presence of cracks in the Pt layer makes it unstable and vulnerable to the acidic atmosphere owing to the exposure of Ni foam and the following chemical reaction i.e. $2\text{H}^+ + \text{Ni} = \text{Ni}^{2+} + \text{H}_2\uparrow$. To fabricate crack-free Pt foams, the introduction of additives to the electrolyte was considered to improve the rigidity of the Pt layer.

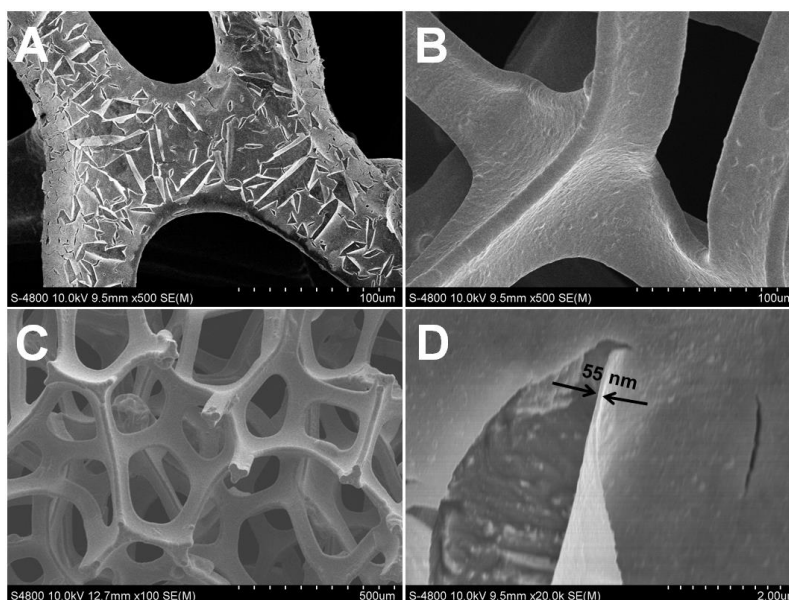


Figure 2. SEM images of Pt foam fabricated using 3 mM H_2PtCl_6 solution without PVP (A), with PVP (B), and Ni foam (C). The thickness of Pt coating on Ni foam electrodeposited for 50 cycles using 0.15 mM PVP in the solution (D).

Inspired by our previous work in which polyvinyl pyrrolidone (PVP, Figure 3A) was utilized for the formation of perpendicular thin-walled Pt nanotubes array through electrodeposition using anodic aluminum oxide (AAO) template [13], we selected PVP as an additive in the electrolyte for the present case. PVP has been extensively used in the synthesis of nanoparticles owing to its inherent properties of chemical stability, water solubility, high polarity, low toxicity, and tackiness. When PVP

(0.15 mM) was introduced into the electrolyte for Pt deposition, CV plot of the Pt foam changed compared to that conducted in the absence of PVP in the electrolyte. The broad peak which appeared between 0 and 0.7 V for 50 cycles of Pt deposition as shown in Figure 1A was of a higher intensity compared to the case where 10 cycles Pt deposition was performed in the presence of PVP containing electrolyte (red curve in Figure 1B). Surprisingly, the broad peak corresponding to 50 cycles deposition using PVP containing electrolyte (blue curve in Figure 1B) disappeared. This implies that the Pt coating fabricated using PVP containing electrolyte was more efficient and crack-free for small duration of deposition. Meanwhile, the SEM images of Pt foams revealed that Pt coating electrodeposited in the absence and presence of PVP showed distinctly different surface morphologies as shown in Figures 2A and 2B. Pt foam (Figure 2B) electrodeposited for 50 cycles using electrolyte containing 0.15 mM PVP and 3 mM H_2PtCl_6 was crack-free. As observed from Figure 2C, Pt foam produced by PVP-containing electrolyte displayed a morphology and pore size similar to the original Ni foam. This similarity should be ascribed to the nanoscale thickness (~ 55 nm, Figure 2D) of Pt layer that makes thickness change negligible relative to thick ligaments in Ni foam.

3.4 Role of PVP

The probable functions of PVP (see molecular structure in Figure 3A) in the crack-free Pt electrodeposited Ni foam are analyzed in the following paragraph. (i), Linear homopolymer PVP bears hydrophobic alkyl groups in the chain, which is able to repel themselves out of the aqueous solution to the interface between the solid and the liquid, and adsorb on the surface of Ni in the conformation of tails or loops (Figure 3B), or other minor conformations (single-point attachment, multiple site attachment, nonuniform segment distribution, random coil, and multilayer) [19]. This adsorption could minimize the interfacial free energy to make the system more stable [14, 20]. Especially, the adsorption of PVP on the surface of Ni can significantly reduce the higher surface energy of the defective sites, so that the Pt atoms could not be selectively deposited at a higher rate on the specific defective sites but deposit homogeneously. Similarly, PVP in the solution could further decrease the surface energy of electrodeposited Pt clusters leading to the smaller size of Pt clusters that enabled the formation of a more compact Pt coating compared to the larger Pt clusters. (ii) The adsorption of organic PVP molecules decreased the reactivity of the Ni atoms, thus the spontaneous replacement reaction between H_2PtCl_6 and Ni foam was suppressed. Pt atoms could be controlled well by CV deposition technique, resulting in the formation of compact Pt coating free from cracks. To sum up, using such improved electrodeposition method, very thin layers of crack-free Pt could be obtained. Figure 2D shows a Pt foam sample broken deliberately by a pair of tweezers where the ~ 55 nm in thickness of 50 cycles Pt electrodeposition could be observed.

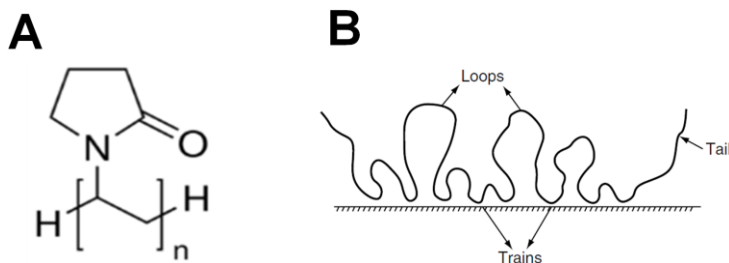


Figure 3. (A) Molecular structure of polyvinylpyrrolidone (PVP), (B) Schematic illustration of conformation of PVP molecule adsorbed on a solid surface.

3.5 Studies on direct methanol fuel cell electrode application

A fuel cell is an electrochemical device that outputs electricity by consuming a chemical fuel. Such energy production releases no or little pollutants to the environment thereby drawing intensive research interest in recent decades in response to the ever-increasing global environmental crisis owing to the combustion of fossil fuel. Methanol is one of the most fundamental small organic compounds used as the basis of hundreds of chemicals and thousands of daily products. In terms of cost, safety, storage and transportation methanol as a fuel is more suitable compared to hydrogen and ethanol. Direct methanol fuel cell (DMFC) operation requires a catalyst to accelerate the process of chemical conversion to produce flow of electrons. So far, Pt as a *d*-block transition metal is one of the most efficient heterogeneous catalysts in DMFC but suffers from high operating cost due to its limited reserves in the earth. The as-fabricated pseudo Pt foam in this work possesses high surface area, is easy to fabricate, freestanding, and cost-effective and can be potentially applied for methanol electrooxidation. To assess the applicability of the pseudo Pt foam on methanol electrooxidation, we conducted comparative studies using the as obtained Pt foam and commercial Pt/C catalyst.

In an acidic solution, a DMFC involves different chemical reactions at the anode and cathode [21, 22].

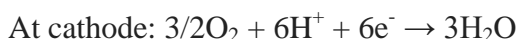
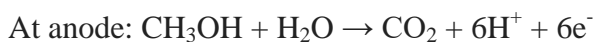


Figure 4A presents cyclic voltammograms of Pt foam in presence and absence of methanol in 0.1 M H₂SO₄. Pt-based catalysts usually exhibit the highest catalytic activity for proton reduction reaction at a very small overpotential. Hence, in acidic solution, hydrogen evolution reaction (HER) occurs theoretically below 0 V (vs SHE) on Pt electrodes resulting in the adsorption of hydrogen on the surface of Pt by forming H–Pt adsorptive bond(s) [23]. The upward and downward peaks between -0.3 and 0.2 V (red curve in Figure 4A) correspond to hydrogen desorption and adsorption, respectively. The upward broad peak at 0.75 V corresponds to the oxygen adsorption to form Pt-O_{ad} and the downward peak at 0.53 V corresponds to the oxygen desorption from Pt-O_{ad}. In the presence of methanol in 0.1 M H₂SO₄, two additional peaks appeared in the CV curve (black curve in Figure 4A). During the forward scan, methanol oxidation peak appeared at 0.66 V and during the backward scan a second methanol oxidation peak appeared at 0.49 V, which corresponds to the oxidation of

intermediate products such as CO and others [24]. All these electrochemical characteristics of pseudo Pt foam matched well with those of Pt/C catalyst in the acidic environment.

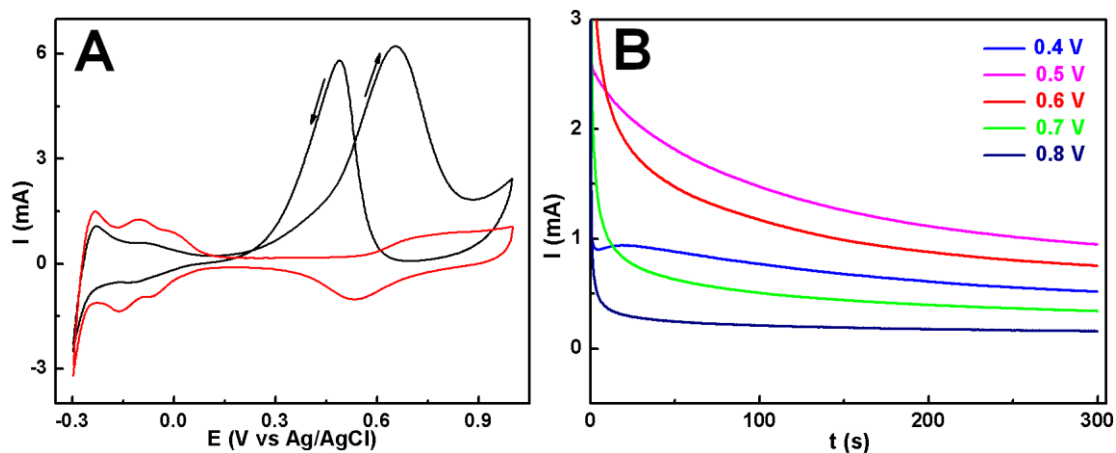


Figure 4. (A) Cyclic voltammograms for Pt foams in presence of methanol (black) and in absence of methanol (red) in 0.1 M H_2SO_4 . (B) Chronoamperometric curves at 0.4, 0.5, 0.6, 0.7, 0.8 V using electrolyte of 0.1 M methanol and 0.1 M H_2SO_4 . Scan rate, 100 mV/s.

Figure 4B shows the chronoamperometric curves for screening the optimum methanol oxidation potential. It was found that 0.5 V could give rise to the highest current of methanol oxidation. Lower or higher potentials produced less current using Pt foam catalyst. Commercial Pt/C electrocatalyst displayed similar voltage-dependent chronoamperometric trend for methanol electrooxidation. The mass of Pt in a Pt foam was obtained by measuring the concentration difference of H_2PtCl_6 in the solution by ICP-AES before and after electrodeposition. Taking into account the factor of mass, Pt foams could produce ca. 48% mass-specific current compared with Pt/C electrocatalyst in the present electrode configuration (Figure 5).

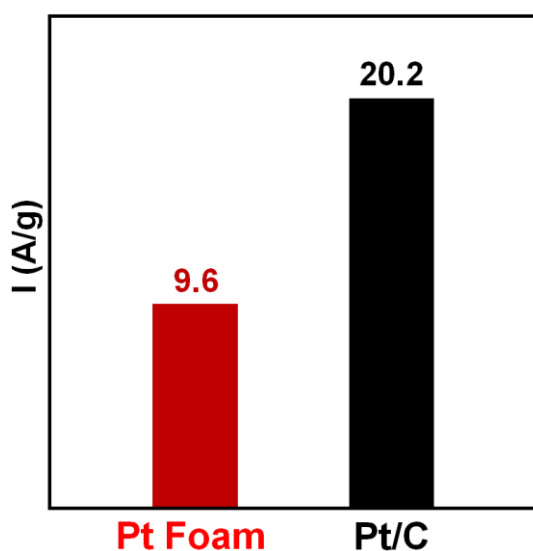


Figure 5. Comparison on mass-specific methanol electrooxidation currents for Pt foam and Pt/C electrocatalysts.

3.6 Comparison of catalytic activity for methanol electrooxidation

The onset potential (0.15 V) of methanol oxidation in the forward scan on pseudo Pt foam is similar to that of Pt/C catalyst, as shown in Fig. 6B. During the backward scan, the Pt/C shows a more negative peak (0.34 vs 0.49 V) than the Pt foam suggesting that the poisoning effect from byproduct intermediates is stronger on Pt/C. From a conventional viewpoint, I_f/I_b (ratio of current densities in forward and backward scan) is one of the important indicators of catalytic performance of a Pt electrocatalyst toward methanol electrooxidation. A large ratio implies good tolerance of the catalyst against the poisoning species generated during methanol electrooxidation. I_f/I_b ratio on Pt/C was 1.9, greater than that on Pt foam, 1.1. Corresponding to this parameter, the commercial Pt/C catalyst showed better tolerance towards intermediate poisoning species. The higher catalytic activity should be attributed to the 0-dimensional and nanoscale Pt particles in the Pt/C electrocatalyst. It is acknowledged that the size of Pt nanoparticle influences its catalytic activity on methanol electrooxidation [25, 26], and the Pt nanoparticles usually exhibit enhanced catalytic activity compared to micro-sized and bulk Pt. The Pt foam fabricated in our work has nanometer thickness but didn't have a nanoscale size along the lateral direction. This is the main reason why catalytic activity of Pt foam was lower than commercial Pt/C catalyst. However, nanoscale Pt coating on three-dimensional interconnected Ni substrate exhibits improved inherent structural stability than dispersed and loosely connected Pt nanopowder. The greatest advantage is that Pt foam structure is devoid of Pt aggregation and subsequent detachment from the substrate electrode.

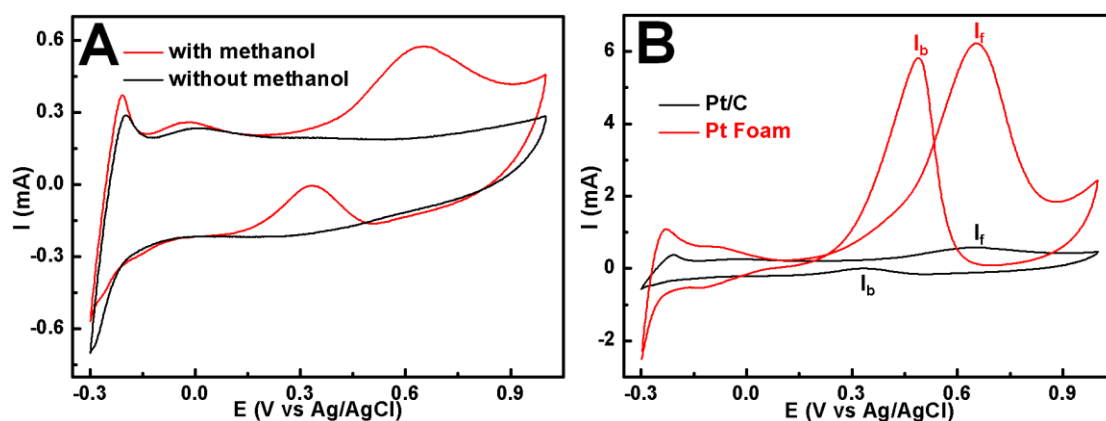


Figure 6. (A) Cyclic voltammograms for commercial Pt/C in absence (black) and presence (red) of methanol in 0.1 M H_2SO_4 . (B) Cyclic voltammograms for Pt/C (red) and Pt foam (black) in 0.1 M H_2SO_4 in presence of 0.5 M methanol.

Catalytic performance was also compared with recent reported Pt-based nanostructures in terms of synthetic simplicity, onset potential, and mass specific current density for methanol electrooxidation (Table 1). As-synthesized pseudo Pt foam cannot exhibit better catalytic performance than reported complex nanostructures but exhibit obvious feature of synthetic simplicity, low cost, acceptable onset potential and current density. As-fabricated Pt foam is more important in the viewpoint of practical use depending on its own distinctive merits.

Table 1. Catalytic performance comparison between pseudo Pt foam and Pt catalyst in literature

Catalyst	Synthetic simplicity/low cost	Onset potential (V)	Current density (A/g)	Reference
Pt/Ti _{0.8} V _{0.2} N	No	0.1	513	[27]
Pd@Pt hexapods	No	~0.35	520	[28]
Pt/MoS ₂ /CN _x	No	0.61	1030	[29]
MWCNTs@SnO ₂ @Pt	No	0.4	1702	[30]
Pt(Mn)/TiC	No	0.39	43	[31]
Pt/HPNC	No	~0.1	700	[32]
Pt foam	Yes	0.15	115	this work

3.7 Stability of Pt foam in acidic solution

Ni is reactive in an acidic solution, hence exposure of Ni to acidic solution can cause instability or breakage. Thus, structural stability of Pt foam is a major concern, and it is necessary to evaluate the stability of Ni based pseudo Pt foam in an acidic solution. In this regard, long duration of CV scans was conducted using 0.1 M H₂SO₄ electrolyte. The peak current of Pt oxide reduction at 0.5 V was indirectly used to evaluate the stability of the Pt foam. Typical CV curves at different scan rates are displayed in Figure 7A. The peak current of Pt-O_{ad} reduction corresponding to the 10th cycle of CV curves (50 mV/s) was acquired for comparison for 10 consecutive days (Figure 7B). The current retained a relatively stable value for 10 days corresponding to a sample immersed in 0.1 M H₂SO₄. This result suggests that Pt foam is stable in acidic solution and the base Ni foam is not exposed.

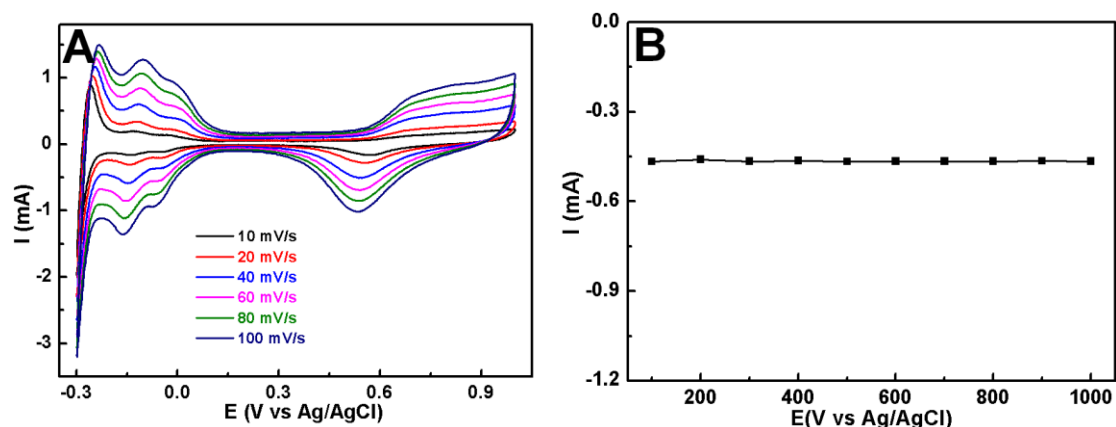


Figure 7. (A) Cyclic voltammograms of Pt foam in 0.1 M H₂SO₄ with different scan rate. (B) Pt foam stability evaluated by observing current level of Pt oxide reduction peak at 0.5 V in CV scan for 10 days.

3.8 Cost consideration

The volume specific current for methanol electrooxidation using the as-fabricated pseudo Pt foam with micron pore size is still not comparable to a foam with nanoscale pore size and a

commercial Pt/C dispersion. But, the cost of Ni foam having micron sized pores is currently much lower because of its large scale industrial use. Furthermore, our homemade solution containing H_2PtCl_6 and PVP for Pt electrodeposition is very simple and cost effective compared with the expensive commercial Pt plating solution. Electrochemical workstation is only main equipment required for the fabrication of Pt foam. Such equipment is inexpensive and working with wet-chemical solution at room temperature, is thus very competitive compared to other fabrication methods such as vacuum sputtering and chemical vapor deposition. With this low-cost strategy, further effort should be invested for achieving smaller pore size of Ni foams, along with the thickness of Pt layer. These depend on the creation of future technological innovations along with cost-centered consideration.

4. CONCLUSIONS

In this work, we successfully fabricated stable and inexpensive pseudo Pt foams by convenient cyclic voltametric deposition of nanoscale Pt layer on Ni foam using a solution of 3 mM H_2PtCl_6 and 0.15 mM PVP. It was found that the presence of PVP in the deposition electrolyte significantly improved the stability of the Pt coating on the Ni foam. The as-fabricated pseudo Pt foam exhibited typical electrochemical characteristics similar to the common commercial Pt/C electrocatalyst. Furthermore, the utility of the Pt foam was successfully demonstrated as a fuel cell catalytic electrode for methanol oxidation, exhibiting high mass specific current relative to commercial Pt/C catalyst. Most importantly, Pt foam may find extensive applications on a commercial scale owing to its low cost and high surface area, as a counter electrode, fuel cell electrode, electrochemical sensor electrode, and corrosion resistive filtration film.

ACKNOWLEDGEMENTS

This work was financially supported by the Zhejiang Provincial Natural Science Foundation of China under grant NO. LY17B010003 and LY15B050005.

References

1. J. Banhart, *Prog. Mater. Sci.*, 46 (2001) 559.
2. L.P. Lefebvre, J. Banhart and D.C. Dunand, *Adv. Eng. Mater.*, 10 (2008) 775.
3. J. Zhang and C.M. Li, *Chem. Soc. Rev.*, 41 (2012) 7016.
4. M.F. Ashby, *Metal Foams: A Design Guide*, Butterworth-Heinemann (2000).
5. J. Banhart, *Adv. Eng. Mater.*, 15 (2013) 82.
6. C.R.K. Rao and D.C. Trivedi, *Coord. Chem. Rev.*, 249 (2005) 613.
7. M. Li, Q. Ma, W. Zi, X. Liu, X. Zhu and S. Liu, *Science Adv.*, 1 (2015) e1400268.
8. Y. Yamauchi, M. Komatsu, A. Takai, R. Sebata, M. Sawada, T. Momma, M. Fuziwara, T. Osaka and K. Kuroda, *Electrochim. Acta*, 53 (2007) 604.
9. S. Adora, Y. Soldo-Olivier, R. Faure, R. Durand, E. Dartyge and F. Baudalet, *J. Phys. Chem. B*, 105 (2001) 10489.
10. A.E. Schweizer and G.T. Kerr, *Inorg. Chem.*, 17 (1978) 2326.
11. Han-Pu Liang, Hui-Min Zhang, Jin-Song Hu, Yu-Guo Guo, Li-Jun Wan and Chun-Li Bai, *Angew.*

- Chem. Int. Ed.*, 43 (2004) 1540.
12. L. Liu, S.-H. Yoo and S. Park, *Chem. Mater.*, 22 (2010) 2681.
 13. Z. Liqiu, K. Sang Min, C. Sanghyun, J. Hee-Jeong, L. Lichun and P. Sungho, *Nanotechnology*, 28 (2017) 035604.
 14. Y. Sun and Y. Xia, *Science*, 298 (2002) 2176.
 15. H. Sun, J. He, J. Wang, S.-Y. Zhang, C. Liu, T. Sritharan, S. Mhaisalkar, M.-Y. Han, D. Wang and H. Chen, *J. Am. Chem. Soc.*, 135 (2013) 9099.
 16. Y.G. Sun, B. Mayers, T. Herricks and Y.N. Xia, *Nano Lett.*, 3 (2003) 955.
 17. Y. Xiong, H. Cai, B.J. Wiley, J. Wang, M.J. Kim and Y. Xia, *J. Am. Chem. Soc.*, 129 (2007) 3665.
 18. Y. Xiong, J.M. McLellan, J. Chen, Y. Yin, Z.-Y. Li and Y. Xia, *J. Am. Chem. Soc.*, 127 (2005) 17118.
 19. K. Ishiduki and K. Esumi, *J. Colloid Interface Sci.*, 185 (1997) 274.
 20. L. Gargallo and E. Cid, *Colloid. Polym. Sci.*, 255 (1977) 556.
 21. E. Antolini, T. Lopes and E.R. Gonzalez, *J. Alloys Compd.*, 461 (2008) 253.
 22. M. Winter and R.J. Brodd, *Chem. Rev.*, 104 (2004) 4245.
 23. J. Lipkowsky, P.N. Ross, *Electrocatalysis*, Wiley-VCH, Inc. (1998)
 24. X. Zhao, M. Yin, L. Ma, L. Liang, C. Liu, J. Liao, T. Lu and W. Xing, *Energy Environ. Sci.*, 4 (2011) 2736.
 25. S. Park, Y. Xie and M.J. Weaver, *Langmuir*, 18 (2002) 5792.
 26. C.-C. Ting, C.-H. Liu, C.-Y. Tai, S.-C. Hsu, C.-S. Chao and F.-M. Pan, *J. Power Sources*, 280 (2015) 166.
 27. M. Huang, J. Zhang, C. Wu and L. Guan, *ACS Appl. Mater. Inter.*, 9 (2017) 26921.
 28. A. Jiang, B. Zhang, Y. Xue, Y. Cheng, Z. Li and J. Hao, *Micropor. Mesopor. Mat.*, 248 (2017) 99.
 29. Park, H.-U., E. Lee and Y.-U. Kwon, *Int. J. Hydrog. Energy*, 42 (2017) 19885.
 30. B. Tang, Y. Lin, Z. Xing, Y. Duan, S. Pan, Y. Dai, J. Yu and J. Zou, *Electrochim. Acta*, 246 (2017) 517.
 31. B. Zhang, Z. Pan, K. Yu, G. Feng, J. Xiao, S. Wu, J. Li, C. Chen, Y. Lin, G. Hu and Z. Wei, *J. Solid State Electr.*, 21 (2017) 3065.
 32. Y. Xiong, Y. Ma, J. Li, J. Huang, Y. Yan, H. Zhang, J. Wu and D. Yang, *Nanoscale* 9 (2017) 11077.

© 2017 The Authors. Published by ESG (www.electrochemsci.org). This article is an open access article distributed under the terms and conditions of the Creative Commons Attribution license (<http://creativecommons.org/licenses/by/4.0/>).